Wettabilities of Self-Assembled Monolayers on Gold Generated from Progressively Fluorinated Alkanethiols

Ramon Colorado, Jr. and T. Randall Lee*

Department of Chemistry, University of Houston, 4800 Calhoun Road, Houston, Texas 77204-5003

Received August 8, 2002. In Final Form: December 10, 2002

The conformational order and wettability of self-assembled monolayers (SAMs) on gold generated from a series of partially fluorinated alkanethiols ($F(CF_2)_n(CH_2)_{11}SH$, $n = 1-10$; F*n*H11SH, H11 series), possessing methylene spacers of equivalent length, and the corresponding *n*-alkanethiol (F0H11SH) were characterized by polarization modulation infrared reflection absorption spectroscopy (PM-IRRAS) and contact angle goniometry. The PM-IRRAS analyses revealed that the conformational order of the underlying methylene spacers remains constant with increasing *n*. Probing the wettabilities of the SAMs by contact angle goniometry using hydrocarbon and fluorocarbon contacting liquids revealed that the dispersive surface energies of the monolayers decreased as *n* increased from 0 to 6 and then remained constant for $n = 6-10$. Using *cis*-perfluorodecalin as the contacting liquid revealed that the decrease in the dispersive surface energies is due to a decrease in the surface density of the CF_3 groups that occurs as the length of the perfluorocarbon segment increases with increasing *n*. The contact angles of the hydrocarbon liquids revealed that the presence of underlying CF_2 groups can further reduce the strength of the dispersive interactions at the surface. The contact angles of polar contacting liquids on the SAMs were consistent with an increase in the distance of the oriented fluorocarbon−hydrocarbon (FC−HC) dipoles from the monolayer surface with increasing *n*. Calculation of the works of adhesion supported this model. Comparison of the data measured for SAMs derived from the H11 series to those measured for SAMs derived from a series of partially fluorinated alkanethiols whose total chain lengths were held constant (F*n*H*m*SH; $n = 1-10$, $m = 15-6$, respectively; $n + m = 16$; C16 series) and the corresponding *n*-alkanethiol (F0H15SH) revealed that differences in underlying monolayer structure fail to significantly influence the interfacial wettabilities of all of the contacting liquids. Calculation of the dispersive surface energies of the SAMs using the methods of both Zisman and Good, Girifalco, and Fowkes (GGF) revealed that both methods underestimate the energies of fluorocarbon surfaces when hydrocarbon contacting liquids are used, with Zisman's method providing lower estimates, compared to the energies estimated using a fluorocarbon contacting liquid in the GGF method. Overall, the results demonstrate that substituting fluorocarbon segments ($n \geq 6$) for the terminal hydrocarbon segments in alkanethiol SAMs produces lower energy surfaces having wettabilities that are less sensitive to the underlying film structure.

Introduction

Fluorinated organic materials are found in an assortment of everyday industrial and household applications due, at least in part, to their unique interfacial properties (e.g., wettability, friction, and adhesion).[1] Furthermore, fluorinated coatings are used to generate surfaces that are not only remarkably hydrophobic but also extremely oleophobic.[2] Recently, researchers have sought to correlate these interfacial properties with the composition and structure of the molecules that comprise the materials by studying self-assembled monolayers (SAMs) of partially fluorinated alkanethiols (PFAs) ($F(CF_2)_n(CH_2)_mSH$; F*n*H*m*SH) on gold.[3−23] These monolayers (e.g., see Figure 1) consist of an outermost fluorocarbon region, wherein the thickness depends on the length of the fluorocarbon segment, *n*, separated from the innermost S−Au binding region by a hydrocarbon region, wherein the thickness

* Corresponding author. E-mail: trlee@uh.edu.

(1) Garbassi, F.; Morroca, M.; Occhiello, E. *Polymer Surfaces*; Wiley: Chichester, 1994.
(2) Castner, D. G.; Grainger, D. W. *Fluorinated Surfaces, Coatings, and Films*; ACS Symposium Series 787; American Chemical Society: Washington, DC, 2001.
(3) Chidsey, C. E. D.; Loiacono, D. N. *Langmuir* **1990**, *6*, 682.
(4) Hoffman, C. L.; Tsao, M.-W.; Rabolt, J. F.; Johnson, H.; Castner, D. G.; Erdelen, C.; Ringsdorf, H. *Langmuir* **1997**, *13*, 4317.
(5) Schonherr, H.; Vansco, G. J. *Langmuir* **1997**, *13*, 3769.
(6) Schonherr, H.; Vansco, G. J. *Mater. Sci. Eng. C* **1999**, *8*−*9*, 243.
(7) Tsao, M. W.; Hoffman, C. L.; Rabolt, J. F.; Johnson, H. E.; Castner, D. G.; Erdelen, C.; Ringsdorf, H. *Langmuir* **1997**, *13*, 4317.
(8) Tsao, M.-W.; Rabolt, J. F.; Schonherr, H.; Castner, D. G. *Langmuir* **2000**, *16*, 1734.
(9) Kim, H. I.; Koini, T.; Lee, T. R.; Perry, S. S. *Langmuir* **1997**, *13*, 7192.
(10) Kim, H. I.; Koini, T.; Lee, T. R.; Perry, S. S. *Tribol. Lett.* **1998**, *4*, 137.
(11) Miura, Y. F.; Takenaga, M.; Koini, T.; Graupe, M.; Garg, N.; Graham, R. L.; Lee, T. R. *Langmuir* **1998**, *14*, 5821.
(12) Graupe, M.; Koini, T.; Kim, H. I.; Garg, N.; Miura, Y. F.; Takenaga, M.; Perry, S. S.; Lee, T. R. *MRS Bull.* **1999**, *34*, 447.
(13) Graupe, M.; Koini, T.; Kim, H. I.; Garg, N.; Miura, Y. F.; Takenaga, M.; Perry, S. S.; Lee, T. R. *Colloids Surf., A* **1999**, *154*, 239.
(14) Kim, H. I.; Graupe, M.; Oloba, O.; Koini, T.; Imaduddin, S.; Lee, T. R.; Perry, S. S. *Langmuir* **1999**, *15*, 3179.
(15) Colorado, R., Jr.; Graupe, M.; Takenaga, M.; Koini, T.; Lee, T. R. *Mater. Res. Soc. Symp. Proc.* **1999**, *546*, 237.
(16) Graupe, M.; Takenaga, M.; Koini, T.; Colorado, R., Jr.; Lee, T. R. *J. Am. Chem. Soc.* **1999**, *121*, 3222.
(17) Colorado, R., Jr.; Lee, T. R. *J. Phys. Org. Chem.* **2000**, *13*, 796.
(18) Fukushima, H.; Seki, S.; Nishikawa, T.; Takiguchi, H.; Tamada, K.; Abe, K.; Colorado, R., Jr.; Graupe, M.; Shmakova, O. E.; Lee, T. R. *J. Phys. Chem. B* **2000**, *104*, 7417.
(19) Frey, S.; Heister, K.; Zharnikov, M.; Grunze, M.; Colorado, R., Jr.; Graupe, M.; Shmakova, O. E.; Lee, T. R. *Phys. Chem. Chem. Phys.* **2000**, *2*, 1979, 3721.
(20) Frey, S.; Heister, K.; Zharnikov, M.; Grunze, M.; Tamada, K.; Colorado, R., Jr.; Graupe, M.; Shmakova, O. E.; Lee, T. R. *Isr. J. Chem.* **2000**, *40*, 81.
(21) Colorado, R., Jr.; Graupe, M.; Kim, H. I.; Takenaga, M.; Oloba, O.; Lee, S.; Perry, S. S.; Lee, T. R. In *Interfacial Properties on the Submicron Scale*; Frommer, J. E., Overney, R., Eds.; ACS Symposium Series 781; American Chemical Society: Washington, DC, 2001; p 58.
(22) Colorado, R., Jr.; Graupe, M.; Shmakova, O. E.; Villazana, R. J.; Lee, T. R. In *Interfacial Properties on the Submicron Scale*; Frommer, J. E., Overney, R., Eds.; ACS Symposium Series 781; American Chemical Society: Washington, DC, 2001; p 276.
(23) Tamada, K.; Ishida, T.; Knoll, W.; Fukushima, H.; Colorado, R., Jr.; Graupe, M.; Shmakova, O. E.; Lee, T. R. *Langmuir* **2001**, *17*, 1913.

10.1021/la0263763 CCC: $25.00
Published on Web 03/21/2003

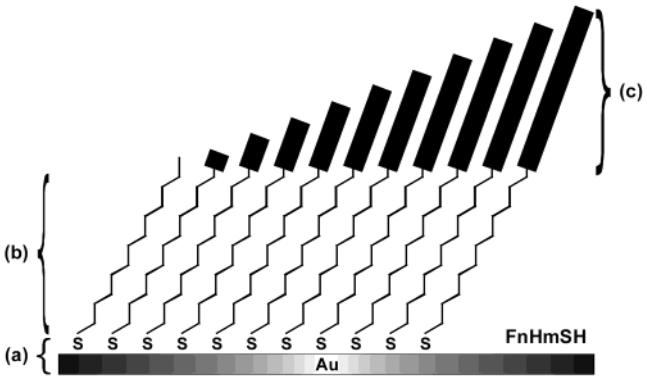

Figure 1. Illustration of the adsorbates on gold that compose F*n*H*m*SH SAMs derived from the H11 series ($n = 0-10$; $m = 11$), depicting (a) the sulfur−gold binding region, (b) the methylene spacers, and (c) the fluorocarbon segments.

depends on the length of the methylene spacer, *m*. SAMs on gold are ideal model systems for investigating fluorinated organic materials because the structure and composition of the films can be controlled at the subnanometer level using routine organic synthetic techniques.[24,25] Moreover, the self-assembly process reproducibly generates robust films that are highly oriented and virtually free of macroscopic defects.[26,27]

Whereas most researchers have focused on examining SAMs formed from a limited number of PFAs,[3−8] our studies in this field have targeted SAMs on gold generated from structurally varied sets of PFAs (F*n*H*m*SH) to investigate in a systematic manner how the lengths of both the fluorocarbon segments and the methylene spacers influence the structure and interfacial properties of the films.[9−23] In studies of wettability, we initially compared SAMs on gold generated from a series of PFAs possessing only terminal trifluoromethyl (CF_3) groups (F1H*m*SH; F1 series) with SAMs on gold generated from a series of the analogous *n*-alkanethiols ($CH_3(CH_2)_mSH$; denoted as F0H*m*SH, where the total number of carbon atoms corresponds to $m + 1$).[11−13,15−17] Surprisingly, the presence of the CF_3 groups failed to produce surfaces that were more hydrophobic than their CH_3-terminated counterparts, but instead gave rise to CF_3-CH_2 (FC−HC) surface dipoles that increased the wettabilities of not only polar protic contacting liquids (e.g., water and glycerol) but also polar aprotic contacting liquids (e.g., acetonitrile and DMF). Subsequently, we examined SAMs on gold derived from a series (denoted as the C16 series) of PFAs whose total chain lengths were held constant at 16 carbon atoms (F*n*H*m*SH; $n = 1-10$, $m = 15-6$, respectively; $n + m = 16$) and the corresponding *n*-alkanethiol (F0H15SH) to study the influence of burying the FC−HC dipoles beneath the surface.[16,17] Increasing the degree of fluorination (*n*) of the films moved the FC−HC dipoles farther from the interface and consequently decreased their influence on the wettabilities of the polar contacting liquids until the dipoles were undetectable for the more highly fluorinated films.

To evaluate the relationships between wettability and the length of the underlying methylene spacer of highly fluorinated films, we studied SAMs on gold derived from a series of PFAs possessing a constant degree of fluorination and an increasing length of the methylene spacer (F10H*m*SH; $m = 2, 6, 11, 17, 33$; the F10 series).[18] We found that only the wettabilities of the thinnest ($m = 2$) and the thickest ($m = 33$) films were influenced by the length of the methylene spacer. Additionally, we evaluated the conformational order of the underlying methylene spacers in both the C16 series and the F10 series by monitoring the antisymmetric methylene stretching band position ($\nu_a^{CH_2}$) using polarization modulation infrared reflection absorption spectroscopy (PM-IRRAS).[18,22] For both series, the conformational order was observed to increase with increasing *m*, reaching values associated with crystalline trans-extended conformations for $m = 11$ and higher. Furthermore, PM-IRRAS analyses of the fluorocarbon-stretching region of the F10 series revealed that the tilt angle of the perfluorocarbon segments with respect to the surface normal was observed to increase with increasing *m*.[18]

The preceding studies demonstrated that the length of the methylene spacer influences both the crystallinity of the underlying hydrocarbon region and the tilt of the fluorocarbon segments.[18,20,22] We have chosen here to examine the effects of removing this influence on the wettabilities of SAMs on gold by using a series (denoted as the H11 series) of progressively fluorinated PFAs possessing methylene spacers of constant length (F*n*H*m*SH; $n = 1-10$, $m = 11$) and the corresponding *n*-alkanethiol (F0H11SH) to generate the monolayers (see Figure 1). The measured wettabilities of these SAMs should depend solely on the degree of fluorination, since keeping the length of the methylene spacers constant at 11 carbon atoms eliminates the aforementioned structural variations that are dependent solely on the chain length of the hydrocarbon segments.[18,20,22] In this paper, we use contact angle goniometry to probe the wettabilities of SAMs derived from the H11 series with a chosen variety of contacting liquids: nonpolar (heptane, decane, tridecane, hexadecane, *cis*-perfluorodecalin), polar protic (water, glycerol), and polar aprotic (acetonitrile, DMF, DMSO, nitrobenzene) contacting liquids. Furthermore, we used PM-IRRAS to evaluate the conformational order of the methylene spacers.[22]

Experimental Section

Materials and Methods. The strategy used to synthesize the PFAs (F*n*H*m*SH) used in this study has been outlined in a recent report,[28] which also provides analytical data for compounds F1H*m*SH ($m = 11-15$), F*n*H11SH ($n = 2-4$), and F*n*H*m*SH ($n = 2-4$, $m = 14-12$, respectively; $n + m = 16$). Analytical data for compounds F10H11SH and F10H17SH can be found in ref 20, and those for compound F10H6SH can be found in ref. 29. All previously reported compounds, including F6H11SH and F8H11SH,[30] exhibited spectral data consistent with those reported in the indicated references. To illustrate a typical experimental procedure used to prepare the previously unreported compounds used in this study, F*m*H11SH ($m = 5, 7, 9$) and F*n*H*m*SH ($n = 6-9$, $m = 10-7$, respectively; $n + m = 16$), we provide below details of the synthesis of F7H11SH, together with analytical data for all other new compounds. All probe liquids (*n*-heptane (H), *n*-decane (D), *n*-tridecane (TD), *n*-hexadecane (HD), *cis*-perfluorodecalin (PFD), water (W), glycerol (G), acetonitrile (AN), dimethylformamide (DMF), dimethyl sulfoxide

(24) Laibinis, P. E.; Palmer, B. J.; Lee, S.-W.; Jennings, G. K. In *Self-Assembled Monolayers of Thiols*; Ulman, A., Ed.; Thin Films 24; Academic: San Diego, 1998; p 1.
(25) Colorado, R., Jr.; Lee, T. R. In *Encyclopedia of Materials: Science and Technology*; Buschow, K. H. J., Cahn, R. W., Flemings, M. C., Ilschner, B., Kramer, E. J., Mahajan, S., Eds.; Elsevier: Oxford, 2001; Vol. 10, p 9332.
(26) Ulman, A. *An Introduction to Ultrathin Organic Films*; Academic: Boston, 1991.
(27) Schreiber, F. *Prog. Surf. Sci.* **2000**, *65*, 151.
(28) Graupe, M.; Koini, T.; Wang, V. Y.; Nassif, G. M.; Colorado, R., Jr.; Villazana, R. J.; Dong, H.; Miura, Y. F.; Shmakova, O. E.; Lee, T. R. *J. Fluorine Chem.* **1999**, *93*, 107.
(29) Smith, D. L.; Wysocki, V. H.; Colorado, R., Jr.; Shmakova, O. E.; Graupe, M.; Lee, T. R. *Langmuir* **2002**, *18*, 3895.
(30) Naud, C.; Calas, P.; Blancou, H.; Commeyras, A. *J. Fluorine Chem.* **2000**, *104*, 173.

(DMSO), and nitrobenzene (NB)), starting materials, reagents, and *n*-alkanethiols (F0H*m*SH; $m = 11-15$) were the highest purity available from commercial suppliers or were synthesized using common methods.

Synthesis of F7H11SH. A 50-mL Schlenk flask was filled with perfluoroheptyl iodide (6.41 g, 12.9 mmol), 10-undecen-1-ol (2.00 g, 11.7 mmol), and the radical initiator 2,2′-azobisisobutyronitrile (0.08 g, 0.5 mmol). The flask was closed, evacuated until the reactants began to bubble, and refilled with argon. This process was then repeated twice. After an additional evacuation, the reaction mixture was stirred for 3 h at 90 °C. The flask was cooled to room temperature, and another portion of 2,2′-azobisisobutyronitrile (0.03 g, 0.2 mmol) was added. The flask was again evacuated by the aforementioned method, and the mixture was then stirred at 90 °C for an additional 3 h. These additions of radical initiator were continued until the disappearance of the 10-undecen-1-ol (as indicated by ^{1}H NMR spectroscopy). The flask was then cooled to room temperature, and the reaction mixture was dissolved with a mixture of 20 mL of tetrahydrofuran (THF) and 40 mL of glacial acetic acid. Zinc dust (15.3 g, 234 mmol) was added to the flask, and the reaction mixture was stirred for 12 h at room temperature. The mixture was then filtered through Celite. The Celite was rinsed with two 100-mL portions of diethyl ether, and the resulting clear solution was concentrated by rotary evaporation. The residue was dissolved in 200 mL of diethyl ether, and this ethereal solution was rinsed with equivalent volumes of saturated aqueous $NaHCO_3$ and saturated aqueous NaCl, dried with $MgSO_4$, and filtered. After the solvent was removed by rotary evaporation, the crude product was recrystallized from ethanol to give 11-perfluoroheptyl-1-undecanol (2.50 g, 4.62 mmol, 40% yield based on 10-undecen-1-ol). ^{1}H NMR (300 MHz, $CDCl_3$): $\delta = 3.64$ (t, $J = 6.6$ Hz, 2H), 2.20−1.85 (m, 2H), 1.65−1.45 (m, 5H), 1.45−1.20 (m, 14H).

The product, 11-perfluoroheptyl-1-undecanol (2.50 g, 4.62 mmol), was dissolved in a mixture of 100 mL of THF and 200 mL of hexanes. Triethylamine (1.41 g, 13.9 mmol) and methanesulfonyl chloride (1.06 g, 9.24 mmol) were added to the solution, and the reaction mixture was stirred at room temperature for 2 h. The organic mixture was then mixed with 200 mL of water, separated, rinsed with saturated aqueous NaCl, dried with $MgSO_4$, and filtered. The solvent was removed by rotary evaporation to give the crude mesylate, which was subsequently dissolved in a mixture of 100 mL of THF and 200 mL of absolute ethanol. After the addition of potassium thioacetate (0.63 g, 5.5 mmol) to the solution, the mixture was stirred and refluxed for 2 h under argon. The reaction mixture was then cooled to room temperature, combined with 200 mL of water, and extracted with hexanes (3 × 200 mL). After combining the organic portions, the solution was rinsed with 200 mL of saturated aqueous NaCl, dried with $MgSO_4$, and filtered. The solvent was removed by rotary evaporation to give the crude thioacetate, which was subsequently dissolved in 100 mL of THF. This solution was added over 5 min to a suspension of lithium aluminum hydride (0.35 g, 9.2 mmol) in 100 mL of THF. The mixture was then stirred and refluxed under argon for 2 h. The reaction was cooled to 0 °C, and methanol was added dropwise until the evolution of hydrogen ceased. After adding 200 mL of water, concentrated HCl was added dropwise until the aqueous layer was acidic as indicated by litmus paper. The mixture was extracted with diethyl ether (3 × 150 mL). The organic portions were combined and rinsed with 200 mL of water, saturated aqueous $NaHCO_3$, and saturated aqueous NaCl, dried with $MgSO_4$, and filtered. The solvent was removed by rotary evaporation to give the crude product, which was purified by column chromatography on silica gel (hexanes) to give 11-perfluoroheptyl-1-undecanethiol (1.46 g, 2.63 mmol, 57% yield from 11-perfluoroheptyl-1-undecanol).

12,12,13,13,14,14,15,15,16,16,16-Undecafluoro-1-hexadecanethiol (F5H11SH). ^{1}H NMR (300 MHz, $CDCl_3$): $\delta = 2.52$ (q, $J = 7.2$ Hz, 2H), 1.95−2.19 (m, 2H), 1.55−1.73 (m, 4H), 1.21−1.45 (m, 15H). ^{13}C NMR (75.5 MHz, $CDCl_3$): $\delta = 110-120$ (bm, 5C), 34.40, 31.30 (t, $^2J_{CF} = 23$ Hz), 29.70 (2C), 29.60, 29.46, 29.40, 29.32, 28.72, 24.90, 20.27. Chemical shifts in the range $\delta = 110-120$ are characteristic of long perfluorocarbon chains.[31] HRMS Calcd for $C_{16}H_{23}F_{11}S$: 456.1345. Found: 456.1342(2).

(31) Ovenall, D. W.; Chang, J. J. *J. Magn. Reson.* **1977**, *25*, 361.

12,12,13,13,14,14,15,15,16,16,17,17,18,18,18-Pentadecafluoro-1-octadecanethiol (F7H11SH). ^{1}H NMR (300 MHz, $CDCl_3$): $\delta = 2.52$ (q, $J = 7.2$ Hz, 2H), 1.94−2.14 (m, 2H), 1.52−1.68 (m, 4H), 1.17−1.40 (m, 15H). ^{13}C NMR (75.5 MHz, $CDCl_3$): $\delta = 110-120$ (bm, 7C), 34.42, 31.20 (t, $^2J_{CF} = 23$ Hz), 29.84 (2C), 29.69, 29.55, 29.45, 29.41, 28.74, 25.07, 20.65. Anal. Calcd for $C_{18}H_{23}F_{15}S$: C, 38.86; H, 4.17. Found: C, 39.30; H, 4.16.

12,12,13,13,14,14,15,15,16,16,17,17,18,18,19,19,20,20,20-Nonadecafluoro-1-eicosanethiol (F9H11SH). ^{1}H NMR (300 MHz, $CDCl_3$): $\delta = 2.54$ (q, $J = 7.2$ Hz, 2H), 1.92−2.20 (m, 2H), 1.55−1.65 (m, 4H), 1.14−1.44 (m, 15H). ^{13}C NMR (75.5 MHz, $CDCl_3$): $\delta = 110-120$ (bm, 9C), 34.10, 31.50 (t, $^2J_{CF} = 23$ Hz), 29.94 (2C), 29.67, 29.54, 29.44, 29.39, 28.69, 24.08, 20.27. HRMS Calcd for $C_{20}H_{23}F_{19}S$: 656.1217. Found: 656.1210(7).

11,11,12,12,13,13,14,14,15,15,16,16,16-Tridecafluoro-1-hexadecanethiol (F6H10SH). ^{1}H NMR (300 MHz, $CDCl_3$): $\delta = 2.52$ (q, $J = 7.2$ Hz, 2H), 1.94−2.18 (m, 2H), 1.67−1.53 (m, 4H), 1.20−1.44 (m, 13H). ^{13}C NMR (75.5 MHz, $CDCl_3$): $\delta = 110-120$ (bm, 6C), 34.45, 31.20 (t, $^2J_{CF} = 23$ Hz), 29.71, 29.62, 29.51, 29.38, 29.25, 28.70, 24.90, 20.28. HRMS Calcd for $C_{16}H_{21}F_{13}S$: 492.1156. Found: 492.1152(4).

10,10,11,11,12,12,13,13,14,14,15,15,16,16,16-Pentadecafluoro-1-hexadecanethiol (F7H9SH). ^{1}H NMR (300 MHz, $CDCl_3$): $\delta = 2.53$ (q, $J = 7.2$ Hz, 2H), 1.94−2.14 (m, 2H), 1.55−1.67 (m, 4H), 1.21−1.44 (m, 11H). ^{13}C NMR (75.5 MHz, $CDCl_3$): $\delta = 110-120$ (bm, 7C), 34.44, 31.14 (t, $^2J_{CF} = 23$ Hz), 29.57, 29.49, 29.39, 29.19, 28.74, 24.92, 20.59. HRMS Calcd for $C_{16}H_{19}F_{15}S$: 528.0968. Found: 528.0968(0).

9,9,10,10,11,11,12,12,13,13,14,14,15,15,16,16,16-Heptadecafluoro-1-hexadecanethiol (F8H8SH). ^{1}H NMR (300 MHz, $CDCl_3$): $\delta = 2.53$ (q, $J = 7.2$ Hz, 2H), 1.93−2.15 (m, 2H), 1.56−1.67 (m, 4H), 1.19−1.46 (m, 9H). ^{13}C NMR (75.5 MHz, $CDCl_3$): $\delta = 110-120$ (bm, 8C), 34.19, 31.19 (t, $^2J_{CF} = 23$ Hz), 29.45, 29.39, 28.94, 28.74, 25.14, 20.64. HRMS Calcd for $C_{16}H_{17}F_{17}S$: 564.0779. Found: 564.0776(3).

8,8,9,9,10,10,11,11,12,12,13,13,14,14,15,15,16,16,16-Nonadecafluoro-1-hexadecanethiol (F9H7SH). ^{1}H NMR (300 MHz, $CDCl_3$): $\delta = 2.53$ (q, $J = 7.2$ Hz, 2H), 1.95−2.12 (m, 2H), 1.56−1.67 (m, 4H), 1.22−1.50 (m, 7H). ^{13}C NMR (75.5 MHz, $CDCl_3$): $\delta = 110-120$ (bm, 9C), 34.15, 31.20 (t, $^2J_{CF} = 23$ Hz), 29.25, 29.01, 28.40, 24.85, 20.25. HRMS Calcd for $C_{16}H_{15}F_{19}S$: 600.0591. Found: 600.0583(7).

Preparation of SAMs. Gold substrates (∼1 cm × 3 cm) were prepared by thermally evaporating a thin chromium adhesion layer (∼100 Å) onto the surface of polished silicon wafers, followed by thermal evaporation of gold (∼2000 Å). After rinsing with toluene and absolute ethanol, these gold-coated substrates were incubated in ethanolic solutions (1 mM) of the appropriate thiols for at least 24 h. The resultant monolayers were rinsed with a sequence of dichloromethane, toluene, and absolute ethanol, and were then dried under a stream of ultrapure nitrogen immediately prior to characterization.

Infrared Spectroscopy. Polarization modulation infrared reflection absorption spectroscopy (PM-IRRAS) data were collected using a Nicolet Magna 860 Fourier transform infrared spectrometer equipped with a liquid nitrogen cooled mercury−cadmium telluride (MCT) detector and a Hinds PEM-90 photoelastic modulator. The polarization of the infrared light was modulated between s- and p-polarizations at a frequency of 37 kHz and was incident upon the monolayer surfaces at an angle of 80°. The spectra were obtained by collecting 64 scans at a spectral resolution of 4 cm^{-1}. Band positions were measured using Nicolet Omnic 5.1 software and possess an average error of ±0.5 cm^{-1}.

Contact Angle Goniometry. A Matrix Technologies micro-Electrapette 25 was used to dispense the contacting liquids onto the surface of the monolayers. A Ramé Hart Model 100 contact angle goniometer was used to measure contact angles with the pipet tip in contact with the drop. Reported values for each SAM are the average of measurements taken on at least two different slides using a minimum of three drops per slide. Measured contact angles were always within ±1° of the values reported in the figures and tables. Propagating this error through the calculations (vide infra) gave the following uncertainties for the indicated items: ±0.2 mJ m^{-2} for $\gamma_{SV}^{d(FC)}$ and ±1.0 mJ m^{-2} for γ_{LV}^{d}, W_{SL}, and W_{SL}^{p}. The standard uncertainty associated with fitting the

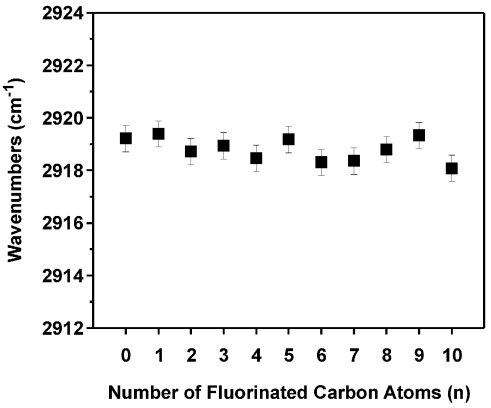

Figure 2. Antisymmetric methylene stretching band position ($\nu_a^{CH_2}$) for the hydrocarbon segments in SAMs derived from the H11 series as a function of the total number of fluorinated carbon atoms per adsorbate (*n*).

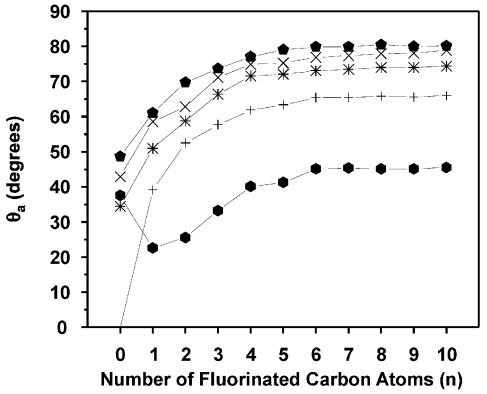

Figure 3. Advancing contact angles of heptane (+), decane (*), tridecane (×), hexadecane (⬟), and *cis*-perfluorodecalin (⬢) on SAMs derived from the H11 series as a function of the total number of fluorinated carbon atoms per adsorbate (*n*).

data using linear regression to calculate $\gamma_{SV}^{d(FC)}$ and $\gamma_C^{(HC)}$ gave uncertainties of ±0.2 mJ m^{-2} and ±2.0 mJ m^{-2}, respectively. Curve fitting of the data was performed with Microsoft Excel XP and Microcal Origin 6.0. The contact angle hysteresis of each monolayer, which is a measure of the surface heterogeneity of the monolayer,[32] was calculated by subtracting the receding contact angles (data not shown) from the advancing contact angles. For a given contacting liquid, there was no observable dependence of contact angle hysteresis on the degree of fluorination. Furthermore, the average contact angle hysteresis of all fluorinated monolayers varied little with the nature of the contacting liquid: H = 10° ± 1°, D = 8° ± 1°, TD = 9° ± 1°, HD = 8° ± 1°, PFD = 10° ± 1°, W = 11° ± 1°, G = 13° ± 1°, AN = 10° ± 1°, DMF = 12° ± 1°, DMSO = 13° ± 2°, and NB = 12° ± 1°. The low absolute values of hysteresis exhibited by all of our monolayers (average hysteresis = 11° ± 1°) are comparable with those previously observed for these contacting liquids on monolayers generated from *n*-alkanethiols on gold and are characteristic of films that possess low surface heterogeneity.[11,32] Therefore, any observed dependence of the wettabilities of the monolayers on the degree of fluorination should be solely attributable to changes in the microscopic local chemical and physical structure of the films and not to the presence of macroscopic regions of chemical or physical heterogeneity on the surface of the films.

Results and Discussion

Infrared Spectroscopy of SAMs. Qualitative differences in the conformational order of the methylene chains in SAMs on gold can be evaluated using infrared (IR) spectroscopy by monitoring the antisymmetric CH_2 stretching band position ($\nu_a^{CH_2}$).[15,22,33] Previous IR studies found that hydrocarbon SAMs with methylene chains composed of 10 or more carbon atoms typically exhibit $\nu_a^{CH_2}$ band positions between 2918 and 2919 cm^{-1}, which is characteristic of predominantly trans-extended crystalline conformations.[22,33] SAMs with shorter methylene chains exhibit $\nu_a^{CH_2}$ band positions at higher frequencies, which is characteristic of less ordered, more liquidlike conformations.[33] Figure 2 shows the $\nu_a^{CH_2}$ band positions for the SAMs derived from the H11 series. As expected due to the constant methylene chain length, all of the SAMs exhibited nearly constant values for $\nu_a^{CH_2}$ (2918.8 ± 0.5 cm^{-1}), indicating that the underlying methylene spacers exist in highly ordered crystalline conformations throughout the entire series.

Wettabilities of SAMs. *Wettabilities Using Nonpolar Contacting Liquids.* Hydrocarbon liquids (e.g., normal alkanes) are the most commonly used contacting liquids in studies of the wetting of "low-energy" surfaces because their completely nonpolar nature makes them excellent probes of the dispersive interactions occurring at the solid−liquid interface.[32] The dispersive interactions between hydrocarbons and fluorocarbons, however, are known to be nonideal.[34−36] For example, *n*-alkane and *n*-perfluoroalkane liquids are immiscible despite the fact that both types of liquids are entirely nonpolar.[34,37−41] To investigate how these phenomena affect the wettabilities of SAMs derived from the H11 series, we measured advancing contact angles (θ_a) using *n*-heptane (H), *n*-decane (D), *n*-tridecane (TD), *n*-hexadecane (HD) (all nonpolar hydrocarbons), and *cis*-perfluorodecalin (PFD) (a nonpolar fluorocarbon) as the contacting liquids (Figure 3). The analysis presented here involves a comparison of experimentally measured contact angles with theoretically predicted contact angles derived from the interfacial energetics of these liquid/surface systems. As will be seen below, the presence of nonideal interactions between the contacting liquids and the monolayer surfaces is most readily apparent in the wettabilities of PFD on the F0H11SH SAM (hydrocarbon surface) and the *n*-alkanes on the F1H11SH SAM (fluorocarbon surface).

Equation 1 shows the Young−Dupré equation,[42−44] which gives the work of adhesion (W_{SL}) (i.e., the work needed to separate an area of liquid from an area of solid) in terms of the surface tension of the liquid (γ_{LV}) and θ_a of the liquid on the solid:

$$W_{SL} = \gamma_{LV}(1 + \cos\theta_a) \quad (1)$$

Equation 2 shows the Good−Girifalco−Fowkes (GGF) equation,[45,46] which relates the work of adhesion to the

(32) Berg, J. C. *Wettability*; Marcel Dekker: New York, 1993.
(33) Porter, M. D.; Bright, T. B.; Allara, D. L.; Chidsey, C. E. D. *J. Am. Chem. Soc.* **1987**, *109*, 3559.
(34) Prior studies have established that the nonideal interactions between comparable hydrocarbons and fluorocarbons are at least partially attributable to dissimilarities in their ionization potentials and molar volumes: (a) Reed, T. M., III. *J. Phys. Chem.* **1955**, *59*, 425. (b) Reed, T. M., III. *J. Phys. Chem.* **1955**, *59*, 428. (c) Scott, R. L. *J. Phys. Chem.* **1958**, *62*, 136.
(35) Chaudhury, M. K. *Mater. Sci. Eng.* **1996**, *R16*, 97.
(36) Drummond, C. J.; Chan, D. Y. C. *Langmuir* **1997**, *13*, 3890.
(37) Mukerjee, P. *Colloids Surf., A* **1994**, *84*, 1.
(38) Riess, J. G. *New J. Chem.* **1995**, *19*, 891.
(39) Sadtler, V. W.; Krafft, M. P.; Riess, J. G. *Angew. Chem., Int. Ed. Engl.* **1996**, *35*, 1976.
(40) Dunitz, J. D.; Taylor, R. *Chem. Eur. J.* **1997**, *3*, 89.
(41) Riess, J. G. *Tetrahedron* **2002**, *58*, 4113.
(42) Young, T. *Miscellaneous Works*; Murray: London, 1855.
(43) Gibbs, J. W. *Collected Works*; Dover: New York, 1961.
(44) Dupré, A. *Théorie Mécanique de la Chaleur*; Paris, 1869.
(45) Good, R. J.; Girifalco, L. A. *J. Phys. Chem.* **1960**, *64*, 561.
(46) Fowkes, F. M. *J. Phys. Chem.* **1963**, *67*, 2538.

dispersive components of the surface free energy of the solid (γ_{SV}^d) and the surface tension of the liquid (γ_{LV}^d):

$$\gamma_{LV}(1 + \cos\theta_a) = 2(\gamma_{SV}^d \gamma_{LV}^d)^{0.5} \quad (2)$$

The GGF equation can be used to predict the contact angles of liquids on SAMs when both γ_{LV} of the contacting liquids and γ_{SV}^d of the SAMs are known, and the interactions at the solid−liquid interface are entirely dispersive. For nonpolar contacting liquids, all of the intermolecular interactions that contribute to the surface tension of the liquid are assumed to be dispersive, so that $\gamma_{LV}^d = \gamma_{LV}$.

Assuming that $\gamma_{LV}^d = \gamma_{LV}$, we previously used eq 2 to estimate an average γ_{SV}^d for a series of F0H*m*SH (*m* = 12−15) SAMs from the contact angles of *n*-alkanes, for which values of γ_{LV} are explicitly known.[17] These manipulations afforded an average value of $\gamma_{SV}^d = 19.7$ mJ m^{-2} for the hydrocarbon SAMs. The literature value of γ_{LV} for PFD is 19.2 mJ m^{-2}.[47] Inserting these two values into eq 2 leads to the prediction that PFD should completely wet the F0H*m*SH SAMs (i.e., θ_a should be 0°). Experimentally, however, PFD exhibits a finite contact angle on these SAMs (average $\theta_a = 38°$). To estimate γ_{LV}^d for this system, we inserted γ_{LV} for PFD (19.2 mJ m^{-2}) and the experimentally measured average θ_a for PFD (38°) into the left side of eq 2 along with γ_{SV}^d(F0H*m*SH SAMs) = 19.7 mJ m^{-2} to give $\gamma_{LV}^d = 15.0$ mJ m^{-2}. Clearly, for PFD, γ_{LV}^d (15.0 mJ m^{-2}) is less than γ_{LV} (19.2 mJ m^{-2}). This discrepancy suggests that only a portion of the intermolecular forces that constitute the surface tension of PFD are utilized when contacting the nonpolar surface of the F0H*m*SH SAMs.

The results for the PFD/F0H*m*SH SAMs system are consistent with previous studies of fluorocarbon/hydrocarbon systems,[36,48−50] which have led to the proposal that the dispersive energies of hydrocarbon surfaces are probed more appropriately with nonpolar hydrocarbon liquids, while the dispersive energies of fluorocarbon surfaces are probed more appropriately with nonpolar fluorocarbon liquids. Indeed, if we assume ideal dispersive interactions between fluorocarbons and hydrocarbons, the use of PFD as the contacting liquid on the hydrocarbon SAMs gives $\gamma_{SV}^d = 15.4$ mJ m^{-2} (calculated by inserting the following values in eq 2: $\gamma_{LV}^d = \gamma_{LV} = 19.2$ mJ m^{-2} and $\theta_a = 38°$), which represents an underestimation of γ_{SV}^d by 4.3 mJ m^{-2}. It is therefore reasonable to anticipate that the interactions between the *n*-alkanes and the fluorocarbon surfaces of F*n*H11SH (*n* = 1−10) SAMs will also be nonideal and will also underestimate the dispersive surface free energies.

This reasoning led us to estimate γ_{SV}^d for a series of F1H*m*SH (*m* = 11−15) SAMs using the average contact angles of PFD ($\theta_a = 24°$) instead of those of the *n*-alkanes to give γ_{SV}^d(F1H*m*SH SAMs) = 17.5 mJ m^{-2}. Using this value and literature values of γ_{LV} for the *n*-alkanes (γ_{LV}(H) = 20.3 mJ m^{-2}, γ_{LV}(D) = 23.9 mJ m^{-2}, γ_{LV}(TD) = 25.9 mJ m^{-2}, γ_{LV}(HD) = 27.5 mJ m^{-2})[32,51] in eq 2, we predict the following contact angles for the *n*-alkanes on the F1H*m*SH SAMs: θ_a(H) = 31°, θ_a(D) = 45°, θ_a(TD) = 50°, and θ_a(HD) = 53°. However, the experimentally measured values of θ_a(H) = 41°, θ_a(D) = 53°, θ_a(TD) = 60°, and θ_a(HD) = 63° are all greater than the predicted values. Calculation of γ_{LV}^d using the experimentally measured θ_a gives γ_{LV}^d(H) = 18.2 mJ m^{-2}, γ_{LV}^d(D) = 21.0 mJ m^{-2}, γ_{LV}^d(TD) = 21.7 mJ m^{-2}, and γ_{LV}^d(HD) = 22.8 mJ m^{-2}. Thus, for all of the *n*-alkanes examined, $\gamma_{LV}^d < \gamma_{LV}$ on the F1H*m*SH SAMs. Therefore, the hydrocarbons appear to interact with the fluorocarbon surfaces using only portions of the intermolecular forces that constitute their surface tensions in a manner similar to that of PFD on the hydrocarbon surfaces.

To rationalize these observations, we considered Fowkes' study of the interfacial interactions between the nonpolar hydrocarbon liquid, squalane, and several liquids having a wide range of polarities.[47] The solubility of nonpolar hydrocarbon liquids (e.g., decalin) in squalane was attributed to the existence of highly favorable dispersive interfacial interactions (i.e., the interfacial tensions between the liquids and squalane equaled zero). Polar liquids, however, exhibited measurable interfacial tensions in squalane due to the existence of nondispersive intermolecular interactions (e.g., acid−base and dipole−dipole interactions) that promote self-association of the polar molecules and thereby discourage dissolution into squalane. Using Fowkes' assumption that the surface free energy of a substance (e.g., the surface tension of a liquid) is the sum of the free energies associated with the individual types of intermolecular interactions present in the substance, one can express the surface tension of a polar liquid as shown in eq 3:

$$\gamma_{LV} = \gamma_{LV}^d + \gamma_{LV}^p \quad (3)$$

where γ_{LV}^p is the polar component of the surface tension that corresponds to the free energy associated with the polar intermolecular interactions.[46] Based on the measured interfacial tensions in squalane, this expression was used to estimate separately the magnitude of the dispersive and polar components of the surface tension of the polar liquids. For example, the known surface tension of water, $\gamma_{LV} = 72.4$ mJ m^{-2}, was separated into $\gamma_{LV}^d = 21.1$ mJ m^{-2} and $\gamma_{LV}^p = 51.3$ mJ m^{-2}, revealing that the majority of the surface tension of water is due to polar self-association interactions.

Fowkes also observed that PFD behaves like a self-associated liquid in squalane, since it was insoluble and exhibited a nonzero interfacial energy.[47] Using Fowkes' system, the surface tension of PFD (19.2 mJ m^{-2}) was separated into $\gamma_{LV}^d = 15.4$ mJ m^{-2} and $\gamma_{LV}^p = 3.8$ mJ m^{-2}. Our measurements for PFD on the hydrocarbon SAMs yielded a similar value for γ_{LV}^d (15.0 mJ m^{-2}; vide supra), which leads to $\gamma_{LV}^p = 4.2$ mJ m^{-2} according to eq 3. Similarly, for each of the *n*-alkanes on the F1H*m*SH SAMs, the use of eqs 1−3 affords the following nonzero values for γ_{LV}^p: 2.1 (H), 2.9 (D), 4.2 (TD), and 4.7 (HD) mJ m^{-2}.

These calculations illustrate that the interactions between fluorocarbons and hydrocarbons are predominantly dispersive in nature; however, the nonzero values of γ_{LV}^p imply that small self-association interactions are manifested when fluorocarbons and hydrocarbons interact. In polar liquids, γ_{LV}^p arises from the existence of true polar intermolecular interactions (e.g., acid−base and dipole−dipole). There is no direct evidence, however, for the existence of analogous interactions in fluorocarbon/hydrocarbon systems that can plausibly give rise to γ_{LV}^p.[47] An alternative explanation, which requires no self-association interactions, is that the values of γ_{LV} for the fluorocarbon or hydrocarbon contacting liquids are simply attenuated when interacting with a hydrocarbon or fluorocarbon surface, respectively, due to an inherent disparity in the nature of fluorocarbon and hydrocarbon dispersive interactions.[34] In other words, a given fluoro-

(47) Fowkes, F. M.; Riddle, F. L., Jr.; Pastore, W. E.; Weber, A. A. *Colloids Surf.* **1990**, *43*, 367.
(48) Fowkes, F. M. *Ind. Eng. Chem.* **1964**, *56*, 40.
(49) Chaudhury, M. K.; Whitesides, G. M. *Langmuir* **1991**, *7*, 1013.
(50) Chaudhury, M. K.; Whitesides, G. M. *Science* **1992**, *255*, 1230.
(51) Jasper, J. J. *J. Phys. Chem. Ref. Data* **1972**, *1* (4), 841.

carbon liquid possesses only dispersive interactions, which act together to totally compose its surface tension γ_{LV}; however, these fluorocarbon dispersive forces are inherently less effective in interacting with the dispersive forces present in hydrocarbons and, as a result, interact with a strength that would correspond to a weaker apparent surface tension γ_{LV}^d. An analogous argument applies to the dispersive interactions that compose the surface tension of a hydrocarbon liquid in contact with a fluorocarbon.

This attenuation factor can be quantified by calculating average ratios of $\gamma_{LV}^d/\gamma_{LV}$, which equal 0.80 for the PFD/F0H*m*SH system and 0.86 for the *n*-alkanes/F1H*m*SH system. These ratios are related to the correction factor (Φ) used in the original Good−Girifalco equation for W_{SL},[45,52] shown in eq 4

$$W_{SL} = 2\Phi(\gamma_{LV}\gamma_{SV})^{0.5} \quad (4)$$

where $\Phi = (\gamma_{LV}^d/\gamma_{LV})^{0.5}$. Values of Φ for the PFD/F0H*m*SH system and the *n*-alkanes/F1H*m*SH system are 0.90 and 0.93, respectively. For reasons discussed below, the dispersive surface energies of the SAMs decrease with increasing *n* and reach constant limiting values for $n = 6-10$. Correspondingly, $\Phi = 0.83$ for the *n*-alkanes/F10H11SH system. Since both hydrocarbon/hydrocarbon systems and fluorocarbon/fluorocarbon systems interact with the full extent of the dispersive interactions that compose their γ_{LV}, no correction factor is needed (i.e., $\Phi = 1$), and eq 4 is equivalent to eq 2 for these systems. Overall, these results support the rule of thumb that fluorocarbons prefer to interact with fluorocarbons and hydrocarbons prefer to interact with hydrocarbons.

As the degree of fluorination (*n*) increases, the contact angles of all of the nonpolar hydrocarbon contacting liquids increase asymptotically (see Figure 3), indicating that the interactions between a given liquid and the surface decrease as the length of the fluorocarbon segment increases until limiting values are met. Zisman observed an analogous phenomenon on SAMs derived from perfluorocarboxylic acids and semifluorinated carboxylic acids on solid substrates.[53−55] In a related study, Johnson and Dettre considered the possible attractive role of the underlying substrate upon the contact angle of the liquids on Zisman's fluorinated SAMs.[56] These authors rationalized the data by proposing that an increase in the length of the fluorocarbon segments would necessarily increase the distance between the contacting liquid and the substrate, which can plausibly lead to a decrease in the attraction between the substrate and the liquid and thus a corresponding increase in the contact angles.

Miller and Abbott offered a similar rationalization to account for the experimentally observed dependence of hexadecane contact angles on the chain length (*m*) of normal alkanethiolate SAMs on gold.[57] Contact angles on SAMs derived from thiols possessing relatively short chain lengths (i.e., $m \leq 9$) are sensitive to the dispersive attraction of the underlying gold substrate, but contact angles on SAMs derived from thiols possessing relatively long chain lengths (i.e., $m > 9$) become insensitive to this attraction and consequently exhibit larger values, which become constant for the longest chain lengths. In our study, the chain length of the shortest adsorbate in the H11 series (F1H11SH) is sufficiently long (12 carbon atoms) to render the influence of the underlying gold substrate negligible. Consequently, the increase in contact angles illustrated in Figure 3 most probably arises from a different source.

Contacting liquids on SAMs are influenced not only by the outermost chemical moieties, but also by the nature of the first few functional groups that lie beneath the monolayer surface.[58,59] Accordingly, the contact angles of nonpolar contacting liquids on the fluorinated SAMs derived from the H11 series (F*n*H11SH; $n = 1-10$) should be influenced by the dispersive nature of the underlying carbon atoms. In this series, the outermost moieties are always CF_3 groups, but the underlying moieties progressively change from methylene ($-CH_2-$) groups to perfluoromethylene ($-CF_2-$) groups as *n* increases. In light of the nonideal dispersive fluorocarbon/hydrocarbon interactions, *n*-alkanes would be expected to interact more strongly with the surface of the F1H11SH SAM compared to the surface of the F10H11SH SAM, because the underlying CH_2 groups of the former offer more attractive dispersive interactions than the underlying CF_2 groups of the latter. Indeed, the observed contact angles for the *n*-alkanes on this series of SAMs increase as *n* increases from 1 to 5 and then become constant for $n = 6-10$, where the contacting liquid can apparently no longer sense the underlying CH_2 groups.

While sensing of the underlying functional groups qualitatively accounts for the observed wettabilities of the *n*-alkanes on the fluorinated SAMs derived from the H11 series, it fails to rationalize the observed wettabilities of PFD on the same series. In keeping with the reasoning proposed above, the interaction between PFD and the surfaces of the SAMs should increase with increasing *n*, since the interaction of PFD with the underlying CF_2 groups of the more fluorinated SAMs is favored over interaction with the CH_2 groups of the less fluorinated SAMs. Nevertheless, the wettability of PFD on these SAMs decreases with increasing *n* (i.e., the contact angles increase with increasing *n*).

Hamaker theory, which models the attractions between macroscopic bodies due to dispersive intermolecular interactions, shows that the dispersive interaction energy of a surface is determined by both the nature of the dispersive field surrounding the individual molecules that comprise the surface and the packing density of the molecules in the surface.[56,60] According to this theory, surfaces that are composed of the same type of molecules (i.e., that possess the same types of dispersive fields) but possess different packing densities of the molecules will exhibit different dispersive interaction energies, with the most densely packed surface exhibiting the largest energy.

(52) Good has proposed that the correction factor, Φ (also known as the interaction parameter), is a function of the ionization potentials, polarizabilities, and dipole moments of the two interacting substances that make up the interfacial system: (a) Good, R. J. *J. Colloid Interface Sci.* **1977**, *59*, 398. (b) Janczuk, B.; Bialopiotrowicz, T. *J. Colloid Interface Sci.* **1990**, *140*, 362. When the two substances possess comparable values of these chemical characteristics, no correction factor for nonideal interactions is needed and $\Phi = 1$. Accordingly, the correction factors estimated for our hydrocarbon/fluorocarbon and fluorocarbon/hydrocarbon systems ($\Phi < 1$) suggest that dissimilarities in the values of these chemical characteristics between hydrocarbons and fluorocarbons can possibly account for the observed deviations from ideal dispersive interactions.[34]

(53) Hare, E. F.; Shafrin, E. G.; Zisman, W. A. *J. Phys. Chem.* **1954**, *58*, 236.

(54) Shafrin, E. G.; Zisman, W. A. *J. Phys. Chem.* **1957**, *61*, 1046.

(55) Shafrin, E. G.; Zisman, W. A. *J. Phys. Chem.* **1962**, *66*, 740.

(56) Johnson, R. E., Jr.; Dettre, R. H. In *Wettability*; Berg, J. C., Ed.; Marcel Dekker: New York, 1993; p 1.

(57) Miller, W. J.; Abbott, N. L. *Langmuir* **1997**, *13*, 7106.

(58) Bain, C. D.; Whitesides, G. M. *J. Am. Chem. Soc.* **1988**, *110*, 5897.

(59) Ulman, A. *Self-Assembled Monolayers of Thiols*; Thin Films 24; Academic Press: San Diego, 1998.

(60) Israelachvili, J. N. *Intermolecular and Surface Forces: With Applications to Colloidal and Biological Systems*; Academic: San Diego, 1985.

These parameters exist in the H11 series, where the packing densities of the fluorinated adsorbates in the F*n*H11SH ($n = 1-10$) SAMs depend on the length of the fluorocarbon segment. Measuring the lattice spacing of SAMs from topographical images obtained using atomic force microscopy (AFM) is the most common method of evaluating the packing density of adsorbates, where larger lattice spacings indicate less densely packed adsorbates.[61] The lattice spacings of F1H*m*SH SAMs are indistinguishable from those of analogous F0H*m*SH SAMs (~5.0 Å),[9,21] indicating that the substitution of a CF_3 group for a CH_3 group on a trans-extended alkyl chain has little effect on the packing of the adsorbates. Adsorbates having longer perfluorinated terminal segments (e.g., perfluorodecyl groups; $F(CF_2)_{10}-$), however, form SAMs on gold with larger lattice spacings (~5.8 Å) as a consequence of the helical structure of perfluoroalkyl chains, which occupy approximately 1.5 times the volume of trans-extended alkyl chains.[62-65]

Taken together, these factors argue that the wettabilities of PFD (and the *n*-alkanes) on the fluorinated SAMs derived from the H11 series should vary as a function of *n*. As *n* increases, the packing densities of the adsorbates (and thus the surface densities of the CF_3 groups) decrease, which consequently lowers the dispersive interaction energies of the surfaces. This decrease in energy reduces the attraction between the contacting liquid and the surface, giving rise to higher contact angles. Like the *n*-alkanes, the contact angles of PFD on this series of SAMs increase as *n* increases from 1 to 5 and then become constant for $n = 6-10$.

To quantify this effect, we calculated the work of adhesion between PFD and the fluorinated SAMs derived from the H11 series using eq 1, and then used nonlinear regression to fit the values as an exponential function of *n*, $W_{SL} = Ae^{(-kn)} + B$, which describes the decrease of W_{SL} from an initial value of $A + B$ to a final asymptotic value of B with a constant k. The work of adhesion decreased with $k = 0.30$ per unit increase in *n*. A corresponding analysis was performed for the contact angles of the *n*-alkanes on this series; for all of the hydrocarbon liquids, the work of adhesion decreased with an average value of $k = 0.51$ per unit increase in *n*. Since only 0.30 of this value can be attributed to the decreased surface density of the CF_3 groups, the difference can plausibly arise from the sensing of the underlying CF_2 groups by the hydrocarbon contacting liquids.

Wettabilities of Polar Contacting Liquids. Figure 4 shows the contact angles of water and glycerol (both polar protic liquids) and acetonitrile, DMF, DMSO, and nitrobenzene (all polar aprotic liquids) on the SAMs derived from the H11 series. The minimum contact angles for each liquid are observed when $n = 1$, which is due to the presence of FC−HC surface dipoles (vide supra); these dipoles interact strongly with the permanent dipoles of the molecules comprising the contacting liquids, and thus lead to enhanced wettabilities.[11-13,15-17] In the more highly fluorinated SAMs (i.e., $n > 1$), the FC−HC dipoles (determined by the location of the CF_2-CH_2 bond) become

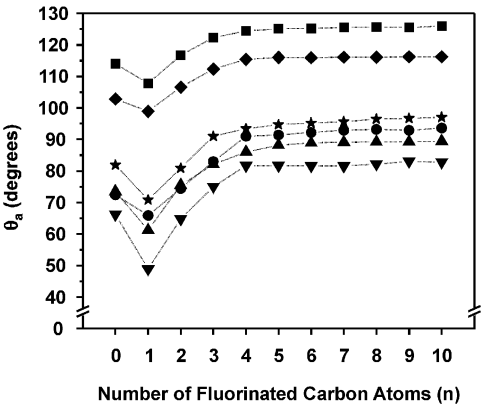

Figure 4. Advancing contact angles of water (■), glycerol (◆), acetonitrile (▼), DMF (▲), DMSO (★), and nitrobenzene (●) on SAMs derived from the H11 series as a function of the total number of fluorinated carbon atoms per adsorbate (*n*).

progressively buried beneath the monolayer surface as *n* increases. We evaluated the influence of this phenomenon on the wettabilities of the SAMs by calculating W_{SL} for each liquid on the SAMs using eq 1 (where γ_{LV} is the literature value of the surface tension of the polar liquids and θ_a is the experimentally measured contact angle) and calculating W_{SL}^d (as detailed below).[17,47] Subtraction of W_{SL}^d from W_{SL} affords W_{SL}^p according to eq 5:

$$W_{SL} = W_{SL}^d + W_{SL}^p \quad (5)$$

The calculation of W_{SL}^d requires knowledge of the dispersive components of the surface tensions (γ_{LV}^d) of the polar contacting liquids and the dispersive components of the surface free energies (γ_{SV}^d) of the SAMs. Fowkes calculated γ_{LV}^d for polar liquids through their interaction with squalane;[47] however, the use of these values in calculations involving fluorinated surfaces might be inappropriate, since the dispersive forces of polar liquids might also interact in a nonideal fashion with the dispersive forces of the fluorinated surfaces. In our case, it was therefore preferable to calculate γ_{LV}^d for the polar liquids through their interactions with fluorinated surfaces.

Utilizing eq 2, we determined average values of γ_{LV}^d for the polar liquids using literature values of γ_{LV} and three highly fluorinated SAMs (F10H*m*SH; $m = 6$, 11, and 17) as the dispersive surfaces instead of squalane.[17,47] As previously indicated, the wettabilities of these three SAMs are indistinguishable,[18] and the contact angles of PFD give rise to an average value of $\gamma_{LV}^d = 13.8$ mJ m^{-2}. Our calculations for the polar liquids gave the following values of γ_{LV}^d (in mJ m^{-2}): γ_{LV}^d(W) = 16.5, γ_{LV}^d(G) = 22.8, γ_{LV}^d(AN) = 16.9, γ_{LV}^d(DMF) = 25.0, γ_{LV}^d(DMSO) = 26.3, and γ_{LV}^d(NB) = 30.8. Values of γ_{SV}^d for the SAMs derived from the H11 series were calculated from eq 2 using the contact angles of PFD for the fluorinated SAMs (F*n*H11SH; $n = 1-10$) and the contact angles of the *n*-alkanes for the SAM derived from F0H11SH.

Given these values for γ_{SV}^d and γ_{LV}^d, we then calculated W_{SL}^d using eq 2 [where $W_{SL}^d = 2(\gamma_{SV}^d \gamma_{LV}^d)^{0.5}$], W_{SL} using eq 1, and then W_{SL}^p using eq 5. Figure 5 plots W_{SL}^d and W_{SL}^p for SAMs derived from the H11 series as a function of *n*; these data are presented numerically in Table 1. The values for the F0H11SH SAM show that the work of adhesion on the nonpolar hydrocarbon surface is determined entirely by the dispersive forces that contribute to W_{SL}^d (i.e., $W_{SL}^p = 0$). The presence of the FC−HC dipoles at the outermost surface of the F1H11SH SAM gives rise

(61) Ulman, A. *Characterization of Organic Thin Films*; Butterworth-Heinemann: Boston, 1995.
(62) Alves, C. A.; Porter, M. D. *Langmuir* **1993**, *9*, 3507.
(63) Liu, G.-Y.; Fenter, P.; Chidsey, C. E. D.; Ogletree, D. F.; Eisenberger, P.; Salmeron, M. *J. Chem. Phys.* **1994**, *101*, 4301.
(64) Schonherr, H.; Vansco, G. J. In *Fluorinated Surfaces, Coatings, and Films*; Castner, D. G., Grainger, D. W., Eds.; ACS Symposium Series 787; American Chemical Society: Washington, DC, 2001; p 15.
(65) Analysis of the H11 series by AFM demonstrates that the lattice spacings increase from ~5.0 to ~5.8 Å with increasing *n*: Yam, C. M.; Colorado, R., Jr.; Perry, S. S.; Lee, T. R., manuscript in preparation.

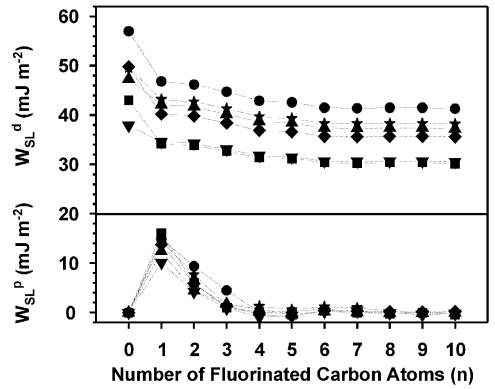

Figure 5. Dispersive works of adhesion (W_{SL}^{d}; upper) and polar works of adhesion (W_{SL}^{p}; lower) of water (■), glycerol (◆), acetonitrile (▼), DMF (▲), DMSO (★), and nitrobenzene (●) on SAMs derived from the H11 series as a function of the total number of fluorinated carbon atoms per adsorbate (n).

Table 1. Works of Adhesion (mJ m^{-2}) for Polar Liquids on Progressively Fluorinated SAMs Derived from the H11 Series

	F0	F1	F2	F3	F4	F5	F6	F7	F8	F9	F10
W_{SL}(W)	43	50	40	34	31	31	31	30	30	30	30
W_{SL}^{d}(W)	43	34	34	33	31	31	31	30	30	30	30
W_{SL}^{p}(W)	0	16	6	1	0	0	0	0	0	0	0
W_{SL}(G)	50	54	46	40	37	36	36	36	36	36	36
W_{SL}^{d}(G)	50	40	40	38	37	36	36	36	36	36	36
W_{SL}^{p}(G)	0	14	6	1	0	0	0	0	0	0	0
W_{SL}(AN)	38	45	38	34	31	31	31	31	31	30	30
W_{SL}^{d}(AN)	38	35	34	33	31	31	31	31	31	30	30
W_{SL}^{p}(AN)	0	10	4	1	0	0	0	0	0	0	0
W_{SL}(DMF)	47	55	46	42	39	38	38	37	37	37	37
W_{SL}^{d}(DMF)	47	42	42	40	39	38	38	37	37	37	37
W_{SL}^{p}(DMF)	0	12	4	2	0	0	0	0	0	0	0
W_{SL}(DMSO)	50	58	50	43	41	40	40	39	39	38	38
W_{SL}^{d}(DMSO)	50	43	43	41	41	40	40	39	39	38	38
W_{SL}^{p}(DMSO)	0	15	8	1	0	0	0	0	0	0	0
W_{SL}(NB)	57	62	56	49	43	43	42	42	41	41	41
W_{SL}^{d}(NB)	57	47	46	45	43	43	42	42	41	41	41
W_{SL}^{p}(NB)	0	15	9	4	0	0	0	0	0	0	0

to maximum contributions of W_{SL}^{p} to the works of adhesion, which reflect the strengths of the liquid−surface dipole−dipole interactions. As the FC−HC dipoles are shifted further beneath the surface with increasing n, the values of W_{SL}^{p} reach zero, showing that the influence of the surface dipoles on the liquids diminishes, and ultimately the works of adhesion become solely dependent on the dispersive forces that compose W_{SL}^{d}. It is interesting to note that the values of W_{SL}^{d} for all of the polar liquids exhibit a steady decrease for the series $n = 1-6$. It is likely that this decrease merely reflects the decreasing surface density of the CF_3 groups that is concomitant with increasing n.[65] Nonlinear regression shows that this trend also exhibits an average exponential decrease with $k = 0.30$ per unit increase in n.

SAMs Derived from the H11 Series versus the C16 Series. We compared the data collected for the SAMs derived from the H11 series to those previously collected for the SAMs derived from the C16 series to determine whether the aforementioned differences in structure (e.g., conformational order of the methylene spacers and/or tilt of the fluorocarbon segments) give rise to differences in wettabilities.[17,22] In one previous study,[17] we calculated values of the Zisman critical surface tension (γ_C) and the GGF-determined dispersive surface energy (γ_{SV}^{d}), which were both based on the contact angles of n-alkanes for the SAMs derived from the C16 series, since these quantities are commonly used to estimate the interfacial energies of "low-energy" surfaces. In the present study, we perform similar calculations for the SAMs derived from the H11 series using the contact angle data for the n-alkanes from Figure 3. Table 2 shows values of $\gamma_C^{(HC)}$ (where the superscript "(HC)" indicates that the values were determined using the n-alkanes as the dispersive probes) and values of γ_{SV}^{d}, which were determined using either n-alkanes ($\gamma_{SV}^{d(HC)}$) or PFD ($\gamma_{SV}^{d(FC)}$) as the dispersive probes for the SAMs derived from both the H11 series and the C16 series. The data show that the surface energies of all of the SAMs decrease with increasing n. Small variations in the absolute values of these energies, however, are due to differences in the calculation methods, which are discussed in detail below.

Table 2. Estimated Surface Energies (mJ m^{-2}) of SAMs Derived from the H11 Series (FnH11SH) and the C16 Series (FnHmSH; $n + m = 16$)

n	$\gamma_C^{(HC)}$ (H11)	$\gamma_C^{(HC)}$ (C16)	$\gamma_{SV}^{d(HC)}$ (H11)	$\gamma_{SV}^{d(HC)}$ (C16)	$\gamma_{SV}^{d(FC)}$ (H11)	$\gamma_{SV}^{d(FC)}$ (C16)
0	20.0	20.0	19.4	19.3	15.4	15.3
1	14.9	14.0	15.5	14.7	17.8	17.3
2	9.5	9.5	13.3	12.4	17.4	16.2
3	7.2	7.9	11.6	11.4	16.2	15.9
4	4.8	5.6	10.5	10.3	15.0	14.7
5	4.6	5.0	10.2	10.2	14.7	14.7
6	2.9	5.1	9.9	9.8	14.0	14.4
7	2.8	5.1	9.8	9.8	13.9	14.3
8	3.0	5.3	9.7	9.7	14.0	14.1
9	2.9	5.3	9.6	9.6	14.0	14.1
10	2.7	4.4	9.5	9.5	13.9	13.9

The tabulated values of $\gamma_C^{(HC)}$ and $\gamma_{SV}^{d(HC)}$ for a given series were calculated from the same set of θ_a(n-alkane) data, but differ because they are derived from distinct theoretical approaches. For a given surface, $\gamma_C^{(HC)}$ is evaluated by plotting the cosines of θ_a(n-alkane) versus the values of γ_{LV}(n-alkane) and then fitting the data to a straight line with the formula $\cos\theta_a$ = slope × (γ_{LV}) + intercept, which, according to Zisman, is a purely empirical relation that has no foundation in theory.[53−56] By extrapolating to $\cos\theta_a = 1$, $\gamma_C^{(HC)} = \gamma_{LV}$ can be determined.

Alternatively, the GGF theories of dispersive interactions at surfaces (see eqs 1 and 2) show that $\gamma_{SV}^{d(HC)}$ can be evaluated by plotting the cosines of θ_a(n-alkane) versus (γ_{LV}(n-alkane))$^{-0.5}$ and then fitting the data to a straight line with the formula $\cos\theta_a = 2(\gamma_{SV}^{d(HC)})^{0.5}(\gamma_{LV})^{-0.5} - 1$, whose slope yields $\gamma_{SV}^{d(HC)}$ upon simple mathematical manipulation.[17,45−48,56] The H11 and C16 values of $\gamma_C^{(HC)}$ appear to differ for $n = 6-10$, but they are actually statistically indistinguishable, since calculation of the standard errors of the slopes and the intercepts, determined by linear regression, reveals that the calculated values of $\gamma_C^{(HC)}$ possess average errors of ±2.0 mJ m^{-2}. In contrast, fitting the same data with the GGF equation yields values of $\gamma_{SV}^{d(HC)}$ that possess average errors of ±0.2 mJ m^{-2}. Consequently, the only statistically significant differences in values of $\gamma_{SV}^{d(HC)}$ for the H11 and the C16 series occur for $n = 1$ and 2, but these differences are quite small.[66]

As a whole, values of both $\gamma_{SV}^{d(HC)}$ and $\gamma_{SV}^{d(FC)}$ for the H11 series are largely indistinguishable from the respective values for the C16 series,[66] demonstrating that the differences in monolayer structure that exist between the two series fail to produce any substantial differences in the dispersive wetting interactions of the films. The dispersive surface energies of the SAMs derived from the

(66) The surfaces of the F1HmSH and F2HmSH SAMs in the H11 series were slightly more wettable than their counterparts in the C16 series. We are currently investigating the possible influence of the shorter chain lengths of these H11 SAMs on the wettabilities using series of SAMs that possess varying values of m.

C16 series are also insensitive to the influence of the gold substrate, which is reasonable given that the total chain lengths of the adsorbates are 16 carbon atoms.[57] The data show that the dispersive interfacial energies of the SAMs derived from the C16 series are instead influenced by the same phenomena as the SAMs derived from the H11 series, namely decreasing surface density of CF_3 groups and sensing of the underlying CF_2 groups. We compared the contact angles of the polar contacting liquids on the SAMs derived from the H11 series (Figure 4) to the analogous data for the SAMs derived from the C16 series published in a previous study.[17] For a given surface, the measured values of θ_a(polar liquid) differed by no more than $\pm 2.0°$ between the H11 series and the C16 series,[66] demonstrating that the polar wetting interactions of the films are also unaffected by the differences in monolayer structure.

The presence of nonideal dispersive fluorocarbon/hydrocarbon interactions can also be extracted from the data in Table 2. For example, the value of $\gamma_{SV}^{d(FC)}$ for $n = 0$ underestimates the dispersive energy of the hydrocarbon surface. For the remaining SAMs, both $\gamma_C^{(HC)}$ and $\gamma_{SV}^{d(HC)}$ underestimate the dispersive energies of the fluorocarbon surfaces, with Zisman's method giving consistently lower values than the GGF method.

Taking these details into consideration, we propose the following summary of the data. Replacing the CH_3 groups of the F0H*m*SH SAMs with the CF_3 groups of the F1H*m*SH SAMs leads to a decrease of ~ 2 mJ m^{-2} in the dispersive surface energy, suggesting that in these two types of SAMs, which exhibit equivalent terminal group densities (vide supra), the fluorocarbon moieties generate attractive dispersive fields that are slightly weaker than those produced by the hydrocarbon moieties. The further decrease in the dispersive surface energies that occurs with increasing n is due to a decreasing surface density of fluorocarbon groups that accompanies the increasing length (and volume) of the perfluorocarbon segments and becomes constant for $n = 6-10$. The highly fluorinated monolayers ($n = 6-10$) are truly "low-energy" surfaces that possess dispersive surface energies that are substantially lower than those of purely hydrocarbon surfaces. The magnitude of this difference in energy between fluorocarbon and hydrocarbon surfaces is, however, overestimated by only considering the value of either $\gamma_C^{(HC)}$ (~ 16 mJ m^{-2}) or $\gamma_{SV}^{d(HC)}$ (~ 10 mJ m^{-2}). By selecting $\gamma_{SV}^{d(HC)}$ for the hydrocarbon surfaces and $\gamma_{SV}^{d(FC)}$ for the fluorocarbon surfaces as perhaps the most reliable values of surface energy, the more realistic difference in energy might actually be closer to ~ 5 mJ m^{-2}.

Conclusions

SAMs on gold generated from a series of partially fluorinated alkanethiols (F*n*H11SH; $n = 1-10$), possessing methylene spacers of equivalent length, and the corresponding *n*-alkanethiol (F0H11SH) were characterized by PM-IRRAS and contact angle goniometry. The PM-IRRAS measurements demonstrated that the methylene spacers in all of the SAMs possess conformational orders that are similarly crystalline. The contact angles of both hydrocarbon (H, D, TD, HD) and fluorocarbon (PFD) nonpolar contacting liquids increased as n increased from 0 to 6 and then remained constant for $n = 6-10$, reflecting a decrease in the dispersive surface energies that is concomitant with progressive fluorination. The interactions between the *n*-alkanes and the fluorocarbon SAMs and the interactions between PFD and the hydrocarbon SAMs were shown to be nonideal. The strengths of these dispersive fluorocarbon/hydrocarbon interactions, inferred from the works of adhesion, were shown to be $\sim 10-20\%$ weaker than the corresponding fluorocarbon/fluorocarbon or hydrocarbon/hydrocarbon interactions.

The contact angles of PFD on the fluorinated SAMs revealed that the decrease in dispersive surface energies with increasing n is due to a decrease in the surface density of CF_3 groups that occurs as the length and the volume of the perfluorocarbon segments increase. Furthermore, the contact angles of the hydrocarbon contacting liquids were shown to be sensitive to the increase in the number of underlying CF_2 groups, which leads to a further reduction in the strength of the dispersive interfacial interactions.

The contact angles of both polar protic and polar aprotic contacting liquids on the SAMs were shown to be sensitive to the presence of FC−HC surface dipoles. As the distance between these dipoles and the liquid−solid interface was increased, the influence of the dipoles, indicated by the polar works of adhesion, diminished until only purely dispersive interactions remained. Comparison of the data obtained for the SAMs derived from the H11 series and those previously measured for the SAMs derived from the C16 series revealed that differences in the monolayer structure exerted no detectable influence on the interfacial wettabilities of either nonpolar or polar contacting liquids.

The dispersive surface energies of the SAMs were estimated by calculating both Zisman critical surface tensions and Good−Girifalco−Fowkes (GGF) dispersive surface energies. Zisman's method gave values for the fluorinated SAMs that were consistently lower than those obtained by the GGF method. Evaluation of the GGF dispersive surface energies for the fluorinated SAMs using hydrocarbon liquids as the dispersive probes produced values that were lower than those estimated using a fluorocarbon liquid as the dispersive probe. Overall, the results indicate that the substitution of perfluorocarbon segments for hydrocarbon segments in SAMs on gold produces films that possess (1) significantly lower dispersive surface energies and (2) interfacial wettabilities that are substantially less sensitive to the underlying film structure than their hydrocarbon counterparts. Moreover, the results demonstrate that the ability to engineer "low-energy" surfaces characteristic of bulk perfluorocarbon films requires the use partially fluorinated alkanethiols that possess six or more terminal fluorocarbon atoms.

Acknowledgment. The National Science Foundation (DMR-9700662), the Texas Advanced Research Program (003652-0307-2001), and the Robert A. Welch Foundation (E-1320) provided generous support for this research. R.C. kindly thanks the National Research Council−Ford Foundation and the University of Houston Center for Mexican−American Studies for predoctoral fellowships.

LA0263763